Material Science & Engineering Journal

Original Article
Published: 06 Jun, 2017

Synthesis and High Temperature Dielectric and Complex Impedance Spectroscopic Studies of Dense $ZnAl_2O_4$ Ceramics

Buchi Suresh M* and Roy Johnson

Centre for Ceramic Processing, International Advanced Research Centre for Powder Metallurgy and New Materials (ARCI), Balapur, Hyderabad, Telangana, India

Abstract

$ZnAl_2O_4$ spinel ceramics were synthesized by solid state reaction from stoichiometric mixture of precursor oxides such as ZnO and Al_2O_3. Phase pure $ZnAl_2O_4$ powder was compacted and the specimens were subjected to sintering experiments. The dilatometric curves indicated a prominent densification regime. Sintered samples were characterized by XRD, SEM, thermal expansion and high temperature complex impedance spectroscopy. X-ray pattern showed cubic spinel phase with crystallite size of 40 nm. Dilatometric analysis resulted into a thermal expansion of 8.4×10^{-6}/°C (RT-1,000°C). High temperature dielectric and complex impedance spectroscopic analysis of the ceramics have been investigated in the frequency range from 1 Hz to 1 MHz and temperature range from 300°C to 700°C. Experimental results revealed the decrease in dielectric constant (e_r) and real part of impedance (Z') with frequency and an increase in electrical conductivity with frequency. Imaginary part of impedance (Z") reaches to a maximum value with increasing frequency and thereafter decreases with further increase in frequency. The complex impedance analysis suggests predominant conduction is due to grain and grain boundaries. Activation energy obtained from the conductivity plot indicates an Arrhenius type thermally activated process due to oxygen vacancies suggesting the conduction by hopping mechanism. SEM image revealed a highly dense microstructure with well bounded grains with average grain size of 3.5 mm.

Keywords: Dielectric constant; Impedance spectroscopy; Conductivity; Spinel; Thermal expansion

OPEN ACCESS

Correspondence:
Buchi Suresh M, Centre for Ceramic Processing, International Advanced Research Centre for Powder Metallurgy and New Materials (ARCI), Balapur, Hyderabad, Telangana, India, E-mail: suresh@arci.res.in

Received Date: *02 May 2017*
Accepted Date: *29 May 2017*
Published Date: *06 Jun 2017*

Citation:
Buchi Suresh M, Johnson R. Synthesis and High Temperature Dielectric and Complex Impedance Spectroscopic Studies of Dense $ZnAl_2O_4$ Ceramics. Mater Sci Eng J. 2017; 1(1): 1001.

Introduction

Dielectric materials used in the millimeter-wave technology should have the properties of lower dielectric constant (e_r) and higher Quality (Q) [1,2]. The dielectric ceramics with lower dielectric constant can minimize cross coupling with conductions and reduce the electronic signal transition time [3,4]. It is reported that the dielectric constant in the range of 4-12 is used for the millimeter wave applications and as microwave substrates [5].

Zinc aluminate ($ZnAl_2O_4$) is of interest due to its high thermal stability, mechanical resistance and low temperature sinterability. It has unique properties of low dielectric permittivity and high Q. It is also transparent to light above 320 nm due to large optical band gap (3.8 eV) and hence used in optoelectronic, spacecraft application for thermal control coatings and as high temperature ceramic material [6,7]. However, high sintering temperatures (1,650°C and above) restricts its use for real application [8]. In 2008, Chen et al. [3] reported the spinel structure of $ZnAl_2O_4$ by sintering for 4 h at 1,700°C and offered low relative permittivity and high Qxf. Nevertheless, some inherent disadvantages of the spinel structure, particularly high sintering temperature has been restricted the real use of $ZnAl_2O_4$ ceramics. Hence, several approaches have been developed to address this issue [9]. It has been reported that gel-casting decreases the sintering temperature of the ceramics. In addition, it is also found that sintering temperature strongly affects the relative permittivity and it increases with temperature. Moreover, limited literature is available on the room temperature and low temperature electrical and dielectric properties of $ZnAl_2O_4$ spinel ceramics [10].

Hence, in the present work we have systematically investigated the high temperature dielectric and complex impedance spectroscopic properties of $ZnAl_2O_4$ ceramics prepared by conventional solid state sintering method. The mechanisms governing the low dielectric permittivity, grain and grain boundary conduction processes are elucidated.

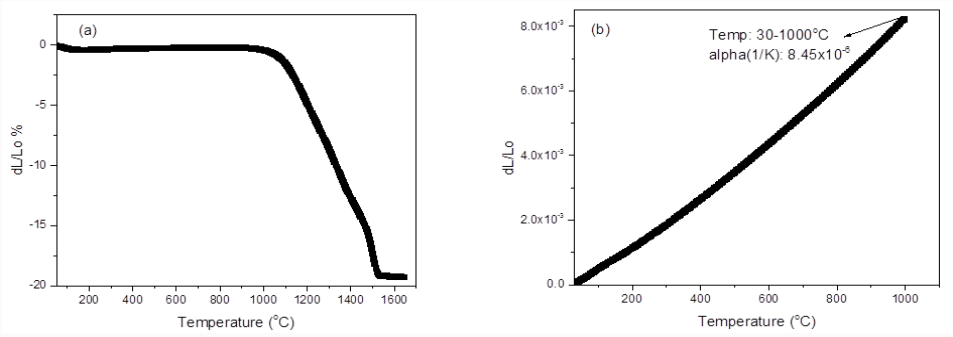

Figure 1: (A) and (B) shows the dilatometric shrinkage for the constant heating rate of 10°C/min and thermal expansion with temperature at a constant heating rate.

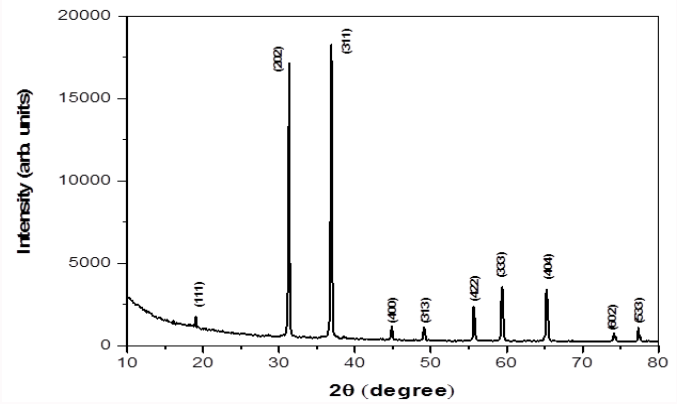

Figure 2: X-ray diffraction pattern of $ZnAl_2O_4$ spinel ceramics.

Experimental

$ZnAl_2O_4$ ceramic samples were synthesized by conventional solid state route. High purity Al_2O_3 (Rohini Industries, Pune, India) and ZnO nano powders were used as starting powders in the required stoichiometry. The mixed powders were wet ball milled with charge to ball ratio of 1:1 for 6 h and dried. Further, the dried powder was calcined at 1,400°C for 1 h and phase formation was confirmed by X-ray diffraction with CuKa radiation (D8-Advanced, Bruker, Germany) and the morphology of the crystalline sample was analyzed using scanning electron microscopy (Hitachi S-3400N, Tokyo, Japan). $ZnAl_2O_4$ powder was ground and granulated by adding 2 wt% of organic binder and pelletized into cylindrical pellets. The pellets with a green density of 48% were subjected to dilatometry in the air using a push rod dilatometer (402C, Netzsch, Germany). The samples are further sintered at 1,550°C for 2 h in a laboratory furnace. Density of the sintered pellets was measured using Archimedes' method with water.

Sintered pellets were characterized by X-ray diffraction with CuKa radiation and scanned through an angular range of 10°<2q>80° with a step size of 0.01°. Further, the thermal expansion behavior of the sample was studied using 25 mm length and 6 mm × 5 mm cross section sample using a dilatometer (NETZSCH 402C Dilatometer) in the temperature regime of room temperature (RT) to 1,000°C. The dielectric and impedance measurements of the samples were measured using an impedance analyzer (SI1260 Solartron, UK). Both the surfaces of the samples were polished and covered with platinum paste. The dried paste was cured at 800°C for 30 min to obtain platinum electrodes. The electroded samples were mounted in the sample holder and placed in the furnace. The temperature is raised by a step of 50°C and the sample is left to stabilize for 15 min before starting the measurement. The data was recorded in the frequency range of 1 Hz to 1 MHz, over a temperature range of 300°C to 700°C and the data analysis was carried out using Z-view software.

Results and Discussion

Dilatometric shrinkage curve of $ZnAl_2O_4$ ceramic is shown in Figure 1A. Sintering behavior of the sample exhibited an onset of shrinkage at a temperature of 1,100°C as is evident from the sudden slope change with a steep shrinkage pattern extending up to 1,550°C. A close to plateau behavior beyond 1,550°C indicates densification regime based on which the sintering temperature is selected as 1,550°C and all the samples were sintered in a laboratory furnace. Thermal expansion in $ZnAl_2O_4$ ceramic is shown in Figure 1B. It is evident from the figure that the coefficient of thermal expansion of the sample is in the range of 8.4×10^{-6}/°C (RT to 1,000°C), which is in good agreement with the earlier studies.

The room temperature XRD of $ZnAl_2O_4$ spinel ceramic is shown in Figure 2. The positions of the peaks were indexed with the standard pattern of JCPDF 65-3104. XRD pattern reveals the spinel cubic structure with maximum intensive (311) peak. No diffraction peaks of other impurity phases were observed, indicating that only $ZnAl_2O_4$ cubic phase has formed. The average crystallite size of the sample was calculated by using Debye Sherrer's formula and is found to be 40 nm [11].

Figure 3A shows the variation in relative permittivity (e_r) as a function of frequency at different temperatures. Relative permittivity is found to decrease significantly with increasing frequency in the low frequency region and remains constant at higher frequencies. In the

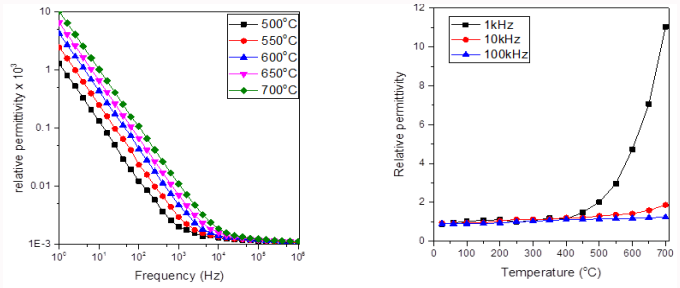

Figure 3: (A) Relative permittivity variation with frequency. (B) Relative permittivity variation with temperature of $ZnAl_2O_4$ spinel ceramics.

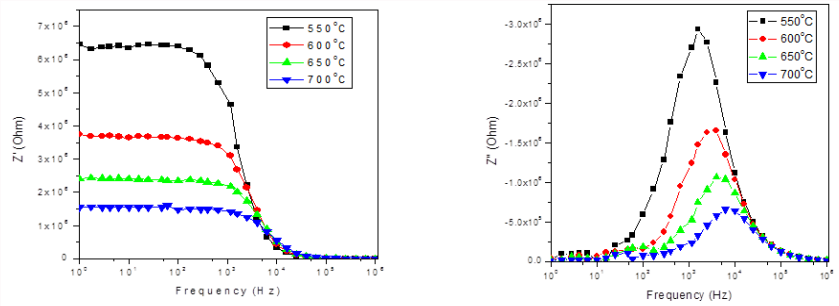

Figure 4: (A) Real part of impedance (Z') versus frequency at different temperatures. (B) Imaginary part of impedance (Z") versus frequency at different temperatures of $ZnAl_2O_4$ spinel ceramics.

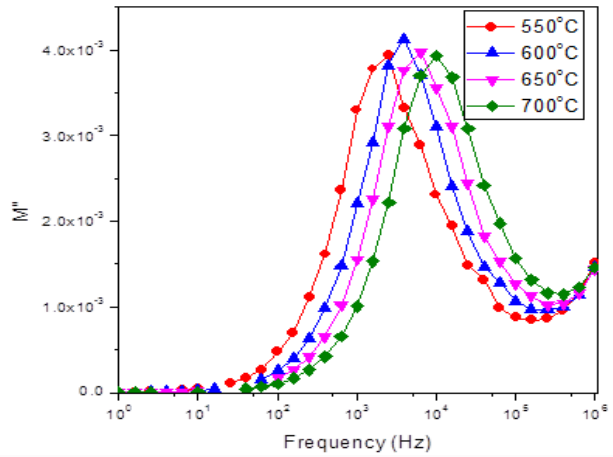

Figure 5: Imaginary part of modulus variation with frequency at different temperatures of $ZnAl_2O_4$ spinel ceramics.

presence of the external electric field, charge carriers can easily move through the grains but accumulated in the grain boundaries. This causes large polarization and enhanced dielectric constant at lower frequencies. In addition, charge carriers cannot migrate through grain boundaries in the low frequency regime and hence the buildup of charge carriers gives rise to polarization, resulting in the higher relative permittivity [12,13]. Temperature dependence of relative permittivity at different frequencies is shown in Figure 3B. From the Figure 3B, it is clear that the relative permittivity is almost constant with an increase in the temperature from room temperature to 400°C and is increased with temperature beyond 400°C.

Figure 4A shows the variation of real part of impedance (Z') at different temperatures as a function of frequency. From the spectra, it is clear that the value of Z' remains constant initially with increase in frequency up to 100 Hz, followed by a sharp decrease in Z' value with further increase in frequency up to 100 kHz and is attributed to the presence of space charges. This may result in the increase in AC conductivity. In addition, the curves merge together in the higher frequency range, suggesting a possible release of space charges in the material. Figure 4B shows the variation of imaginary part of impedance (Z") at different temperatures with increasing frequency. The relaxation peak is observed in the Z" plot and found to shift towards high frequency region with increase in temperature.

To evaluate the nature of relaxation behavior concerning the charge transport mechanism and to distinguish long range conduction from short range hopping motion; frequency dependence on imaginary part of electric modulus (M") is studied. Figure 5 shows the variation of imaginary part of modulus with frequency at different temperatures. Asymmetrically broadened peaks are observed which indicates non-Debye type behavior. In the low frequency range below peak frequency, charge carriers can migrate successfully through hopping from one site to its adjacent site. Beyond the peak frequency,

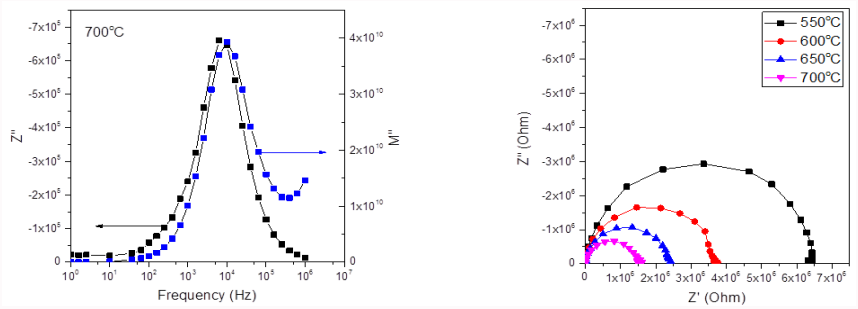

Figure 6: (A) Z" & M" variation with frequency at 700°C. (B) Nyquist plots at different temperatures of $ZnAl_2O_4$ spinel ceramics.

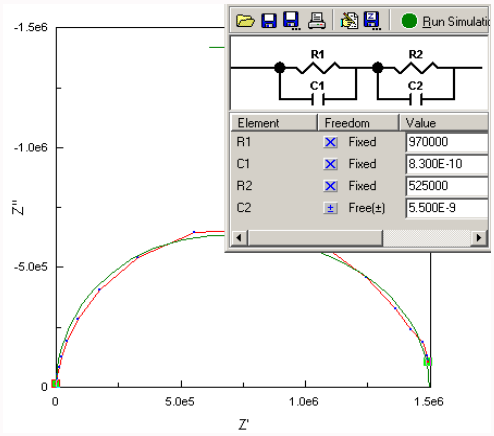

Figure 7: Cole-Cole plot with fitted line and equivalent circuit of $ZnAl_2O_4$ spinel ceramics.

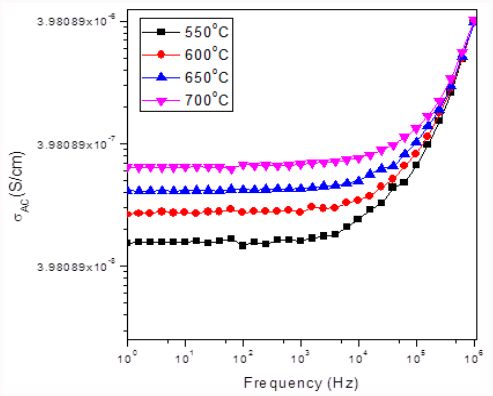

Figure 8: AC conductivity variation with frequency at different temperatures of $ZnAl_2O_4$ spinel ceramic.

the charge carriers are localized and can have short range motion. Further, the peaks are found to shift towards high frequency side with an increase in temperature, indicating the relaxation behavior.

Combined plot of imaginary part of impedance (Z") and modulus (M") with frequency helps to know the presence of low frequency relaxation in the sample. Figure 6A shows the selective plot of impedance (Z") and modulus (M") variation with frequency at 700°C. The maximum values coincide at a particular frequency indicating the similar relaxation process of impedance and modulus spectra. The contribution to multiple relaxation processes such as grain, grain boundary and electrode conduction will be investigated by the analysis of Nyquist plots of impedance. Figure 6B reveals Nyquist plots between the Z" and Z' at different temperatures as a function of frequency. All the plots have resulted into semicircles with a deviation in the low and high frequency regions. From the microstructural point of view, $ZnAl_2O_4$ is a polycrystalline ceramic of grains well separated by grain boundaries. Hence, two semicircles were observed which are ascribed to grain and grain boundaries. The semicircular arc in the lower frequency region is attributed to the grain boundary due to parallel combination of resistance and capacitance. Where, the semicircle in the higher frequency region is due to the grain contribution to the ceramic material.

It is evident from the plots that semicircular arcs at all the temperatures suggest a predominant contribution of grain and grain boundaries. Since the Nyquist plots at all the temperatures are composed of two semicircular arcs and can be expressed as an equivalent circuit made of two parallel RC circuits connected in series. Figure 7 gives the Nyquist plot along with the fitted data taken

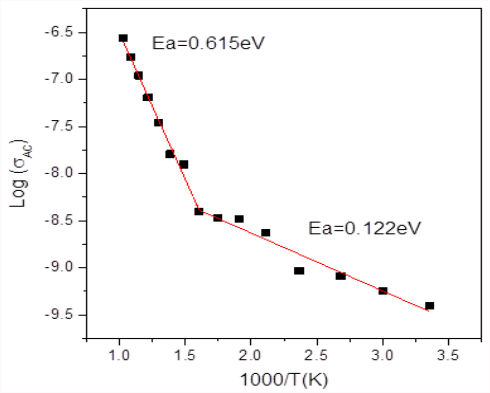

Figure 9: Arrhenius plot of AC conductivity of $ZnAl_2O_4$ spinel ceramics.

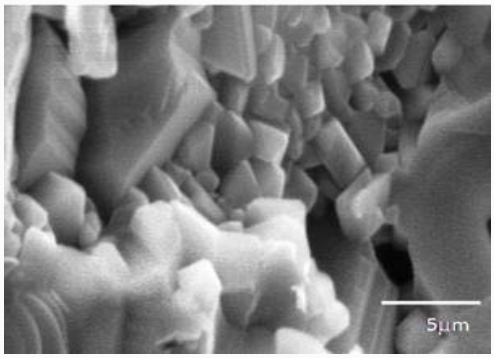

Figure 10: SEM cross section image of $ZnAl_2O_4$ spinel ceramic sample.

over a wider range of frequencies. From the visual inspection of data shown in the figure, it is noted that the Nyquist plot exhibited single depressed semicircular arc which can be fitted to two semicircular arcs with their centers on the axis. This behavior can be modeled well with the series combination of R_1C_1 and R_2C_2, each representing one semicircle. Two RC elements in series are due to the occurrence of two relaxation processes of comparable relaxation times. R_1, C_1 represents the resistance and capacitance of bulk grains and R_2, C_2 represents the resistance and capacitance of grain boundaries.

Figure 8 shows the variation of AC conductivity with frequency from 1 Hz to 1 MHz in the temperature range of 300°C to 700°C. It is evident that electrical conductivity is almost constant in the lower frequency regime and increased gradually with increase in the frequency. At lower frequencies, plateau in conductivity spectra is observed, which might be due to domination of DC conductivity. With increase in the temperature, AC conductivity increases indicating that the conduction is thermally activated. The presence of two slopes suggests that the conduction behavior in the $ZnAl_2O_4$ sample is by the relaxation process occurring at low frequencies due to grain boundaries and charge carriers relaxes at higher frequencies within grains represented by second slope [14]. Thus AC conductivity is proportional to angular frequency in the high frequency region confirming the linear nature.

Figure 9 shows the AC conductivity variation as a function of absolute temperature. From the slopes of the linear fit in the low (RT-300°C) and high (300°C to 700°C) temperature regimes, we can estimate activation energy associated with AC conduction. The activation energy calculated from the slope of the fitted line of the high temperature regime is found to be 0.61eV, which might be due to oxygen vacancies and is in close agreement with the reported values [15-17]. It suggests that the ionic conduction in the $ZnAl_2O_4$ takes place via hopping mechanism. SEM fractured micrograph is show in Figure 10. Image is found to complement well with physico-chemical properties discussed above. SEM image revealed a highly dense microstructure with well bounded grains, though a few isolated pores are observed. The sizes of the grains are found to be fairly uniform and the average grain size is of ~3.5 micron measured using linear intercept method.

Conclusion

Phase pure $ZnAl_2O_4$ spinel ceramics had been successfully synthesized by solid state reaction method as confirmed by XRD results. Dilatometric studies were carried out to arrive at optimum sintering temperature of 1,550°C and sintered sample shown a density of 99% of theoretical density which is complemented by the microstructure. X-ray pattern showed cubic spinel phase with crystallite size of 40 nm. Thermal expansion values were found to be in good agreement with earlier studies. Experimental results revealed the decrease in dielectric constant and real part of impedance (Z') with frequency and an increase in electrical conductivity with frequency. It was found that imaginary part of impedance (Z") reaches a maximum value and thereafter decreases with further increase in the frequency. The complex impedance analysis suggests predominant conduction is due to grain and grain boundaries. SEM image revealed a highly dense microstructure with well bounded grains, though a few isolated pores are observed.

References

1. Tsunooka T, Androu M, Higashida Y, Sugiura H, Ohsato H. Effects

of TiO2 on sinterability and dielectric properties of high-Q forsterite ceramics. J Eur Ceram Soc. 2003;23:2573-8.

2. Kim JC, Kim MH, Lim JB, Nahm S, Paik JH, Kim JH. Synthesis and microwave dielectric properties of Re3Ga5O12 (Re: Nd, Sm, Eu, Dy, Yb, and Y) ceramics. J Am Ceram Soc. 2007;90:641-4.
3. Chen YB, Huang CL, Tasi ST. New dielectric material system of x(Mg0.95Zn0.05Ti)O3–(1 – x)Ca0.8Sm0.4/3TiO3 at microwave frequency. Mater Lett. 2008;62:2454-7.
4. Shin HK, Shin H, Bae ST, Lee S, Hong KS. Effect of oxygen partial pressure during liquid-phase sintering on the dielectric properties of 0.9MgTiO3–0.1CaTiO3. J Am Ceram Soc. 2008;91:132-8.
5. Narang SB, Bahel S. Low loss dielectric ceramics for microwave applications: a review. J Ceram Proc Res. 2010;11:316-21.
6. Sampath SK, Cordaro JF. Optical properties of zinc aluminate, zinc gallate, and zinc aluminogallate spinels. J Am Ceram Soc. 1998;81:649-54.
7. Galetti AE, Gomez MF, Arrúa LA, Abello MC. Hydrogen production by ethanol reforming over NiZnAl catalysts: Influence of Ce addition on carbon deposition. Appl Catal A Gen. 2008;348:94-9.
8. van der Laag NJ, Snel MD, Magusin PCMM, de With G. Structural, elastic, thermophysical and dielectric properties of zinc aluminate (ZnAl2O4). J Eur Ceram Soc. 2004;24:2417-24.
9. Su L, Miao L, Miao J, Zheng Z, Yang B, Xia R, et al. Synthesis and optical property of zinc aluminate spinel cryogels. J Asian Ceram Soc. 2016;4:185-90.
10. All SAE, Fawzy YHA, Radwan RM. Study on the structure and electrical behaviour of zinc aluminate ceramics irradiated with gamma radiation. J Phys D Appl Phys. 2007;40:5707-9.
11. Jamal EMA, Kumar SD, Anantharaman MR. On structural, optical and dielectric properties of zinc aluminate nanoparticles. Bull Mater Sci. 2011;34:251-9.
12. Kiran VS, Sumathi S. Dielectric studies on Bismuth substituted Zinc aluminate Nanoparticles. Intl J Chem Tech Res. 2015;8:97-103.
13. Veena M, Somashekarappa A, Shankaramurthy GJ, Jayanna HS, Somashekarappa HM. Effect of 60Co gamma irradiation on dielectric and complex impedance properties of Dy3+ substituted Ni–Zn nanoferrites. J Mag Mag Mater. 2016;419:375-85.
14. Rekha K, Ahlawat N, Agarwal A, Sanghi S, Sindhu M, Ahlawat N. Rietveld refinement, impedance spectroscopy and magnetic properties of Bi0.8Sr0.2FeO3 substituted Na0.5Bi0.5TiO3 ceramics. J Mag Mag Mater. 2016;414:1-9.
15. Karthik C, Varma KBR. Dielectric and AC conductivity behavior of BaBi2Nb2O9 ceramics. J Phys Chem Solids. 2006;67:2437-41.
16. Raymond O, Font R, Almodovar NS, Portelles J, Siqueiros JM. Frequency-temperature response of ferroelectromagnetic Pb(Fe1⁄2Nb1⁄2)O3Pb(Fe1⁄2Nb1⁄2)O3 ceramics obtained by different precursors. Part I. Structural and thermo-electrical characterization. J Appl Phys. 2005;97:84107.
17. Rao SK, Prasad MD, Krishna MP, Tilak B, Varadarajulu KC. Impedance and modulus spectroscopy studies on Ba0.1Sr0.81La0.06Bi2Nb2O9 ceramic. Mater Sci Eng B. 2006;133:141-50.